# Tracking Deformable Objects with Unscented Kalman Filtering and Geometric Active Contours

Samuel Dambreville, Yogesh Rathi, Allen Tannenbaum

*Abstract*— **Geometric active contours represented as the zero level sets of the graph of a surface have been used very successfully to segment static images. However, tracking involves estimating the global motion of the object and its local deformations as functions of time. Some attempts have been made to use geometric active contours for tracking, but most of these minimize the energy at each frame and do not utilize the temporal coherency of the motion or the deformation. Recently, particle filters for geometric active contours were used for tracking deforming objects. However, the method is computationally very expensive since it requires a large number of particles to approximate the state density. In the present work, we propose to use the unscented Kalman filter together with geometric active contours to track deformable objects in a computationally efficient manner.**

## I. Introduction

The problem of tracking dynamic deformable objects has been a topic of substantial research in the field of controlled active vision; see [1], [2] and the references therein. In this paper, we propose a scheme that combines the advantages of the unscented Kalman filter and geometric active contours (realized via level set models), for dynamic tracking.

In order to appreciate this methodology, we briefly review some previous related work. Various finite dimensional parameterizations of continuous curves have been proposed, perhaps most prominently the B-spline representation used for a "snake model" as in [2]. Isard and Blake (see [1] and references therein) applied the B-spline representation for contours of objects and proposed the Condensation algorithm [3]. The authors in [4], [5] also use B-splines along with the unscented Kalman filter for rigid object tracking. Since these approaches only track the finite dimensional group (e.g., Euclidean, affine) parameters they cannot handle local deformations of the deforming object (see e.g., the fish example in Section IV-A). One possible solution proposed in [6], is to use deformable templates to model prior shapes allowing for many possible deformation modes of shapes.

Another approach for representing contours is via the level set technique [7], [8] which is an implicit representation of contours. For segmenting a shape using level sets, an initial guess of the contour is deformed until it minimizes an image-based energy functional. Different energy functionals which utilize different features of the image have been used in the literature; see e.g. [9], [10], [11], [12]. Some previous work on tracking using level set methods is given in [13], [14], [15], [16].

In [15], the authors propose a definition for motion and shape deformation for a deformable object. Motion is parameterized by a finite dimensional group action while the shape deformation is given by the elastic deformation of the object contour (defined by an infinite dimensional group of diffeomorphisms) modulo the finite dimensional motion group. This is called the *deformotion* model. This approach relies only on the observed images for tracking and does not use any prior information on the dynamics of the group action or of the deformation. As a result it fails if there is an outlier observation or if there is occlusion. To address this problem, in [16], the authors propose a generic local observer to incorporate prior information about the system dynamics in the "deformotion" framework.

Other approaches closely related to our work are given in [2], [17], [18]. Here the authors use a Kalman filter in conjunction with active contours to track nonrigid objects. The Kalman filter was used for predicting possible movements of the object, while the active contours allowed for tracking deformations in the object.

In [19] the authors use particle filters in combination with geometric active contours for tracking deformable objects. Compared with the approach in [19], our method has the advantage of only requiring a small number of deterministic sample points, and is therefore computationally very efficient. It however suffers the limitation of assuming a unimodal probability distribution of the state vector and thus cannot handle multimodal distributions.

This paper is organized as follows: In the next section we discuss the unscented transformation, the unscented Kalman filter, the level set method, and the Chan-Vese model for curve evolution. In Section 3 we describe the state space model and the algorithm in detail. Experimental results are given in Section 4. Limitations and future work are discussed in Section 5.

## II. Preliminaries

In this section, we review some basic notions from the theory of unscented Kalman filtering, as well as level set techniques which we will need in the sequel.

### A. The Unscented Transformation

Julier and Uhlmann [20], [21] proposed a novel approach to generalizing the application of the Kalman filter to nonlinear systems. This approach is based on a statistical technique

Samuel Dambreville, Yogesh Rathi and Allen Tannenbaum are with the School of Electrical & Computer Engineering, Georgia Institute of Technology, Atlanta, GA 30332-0250; {Samuel.dambreville,yogesh.rathi,tannenba}@bme.gatech.edu. This research was supported by grants from NSF, NIH, AFOSR, MURI, HEL-MRI, and ARO.

known as the *unscented transformation.* The unscented transformation leads to a more accurate filter than the traditional Extended Kalman Filter and avoids the costly computation of jacobians [20], [22], [23].

Let $\mathbf{x}$ denote a $n$-dimensional random variable with mean $\hat{\mathbf{x}}$ and covariance $\mathbf{P}$. Let $\mathbf{g}$ be any arbitrary nonlinear function such that $\mathbf{y} = \mathbf{g}(\mathbf{x})$. To calculate the statistics of $\mathbf{y}$ we proceed as follows: A set of $(2n+1)$ weighted points or *sigma points* are deterministically chosen as:

$$\chi_0 = \hat{\mathbf{x}}, \quad \omega_0 = \kappa/(n+\kappa) \tag{1}$$

$$\chi_i = \hat{\mathbf{x}} + (\sqrt{(n+\kappa).\mathbf{P}})_i, \quad \chi_{i+n} = \hat{\mathbf{x}} - (\sqrt{(n+\kappa).\mathbf{P}})_i,$$

$$\omega_i = \omega_{i+n} = 1/\{2(n+\kappa)\}, \quad i = 1, ..., n$$

where, $\kappa$ is a scaling parameter, $(\sqrt{(n+\kappa).\mathbf{P}})_i$ is the $i^{th}$ column of the matrix square root of $(n+\kappa).\mathbf{P}$ and $\omega_i$ is the weight associated with the $i^{th}$ sigma point. Note that $\sum_{i=0}^{2n+1} \omega_i = 1$ and the obtained sigma points have same mean and covariance as $\mathbf{x}$. Each sigma point is now propagated through the nonlinear function: $\gamma_i = g(\chi_i)$ with $i = 0, ..., 2n+1$. The estimated mean and covariance of $\mathbf{y}$ are computed as follows:

$$\hat{\mathbf{y}} = \sum_{i=0}^{2n+1} \omega_i \gamma_i, \quad \mathbf{P}_y = \sum_{i=0}^{2n+1} \omega_i (\gamma_i - \hat{\mathbf{y}})(\gamma_i - \hat{\mathbf{y}})^T$$

### *B. The Unscented Kalman Filter*

Let $\mathbf{x}$(k) denote the $n$-dimensional state at time $k$. The system evolves according to the equation:

$$\mathbf{x}(k+1) = f(\mathbf{x}(k)) + \mathbf{v}(k+1) \tag{2}$$

where $f(.)$ is the state transition function and $\mathbf{v}$(k+1) is a q-dimensional process noise vector. The $m$-dimensional measurement vector $\mathbf{y}$ is linked to the state of the system through the equation:

$$\mathbf{y}(k+1) = h(\mathbf{x}(k+1), \mathbf{u}(k+1)) + \mathbf{w}(k+1) \tag{3}$$

where $h(.)$ is the observation function in which $\mathbf{u}(k+1)$ is new information available at time $(t+1)$ and $\mathbf{w}$(k) is a r-dimensional measurement noise vector. Although more general assumptions about noise can be carried by the unscented Kalman filter, we assume in what follows that, for all integers $(i, j)$:

$$E[\mathbf{v}(k)] = E[\mathbf{w}(k)] = 0 \quad E[\mathbf{v}(i)\mathbf{w}^T(j)] = 0$$

$$E[\mathbf{v}(i)\mathbf{v}^T(j)] = \delta(i,j).\mathbf{Q} \quad E[\mathbf{w}(i)\mathbf{w}^T(j)] = \delta(i,j).\mathbf{R}$$

with $\mathbf{Q}$ and $\mathbf{R}$ being constant matrices of dimensions $(q \times q)$ and $(r \times r)$ respectively. $\mathbf{Q}$ is the process noise covariance matrix, $\mathbf{R}$ is the observation noise covariance matrix. The prediction and update steps of the Kalman filtering algorithm are carried as follows, within the unscented framework:

*1) Prediction:* Assume that the state $\mathbf{x}$(k) at time $t = k$, the corresponding mean $\hat{\mathbf{x}}(k)$ and covariance matrix $\mathbf{P}(k|k)$ are known. The unscented transform is applied to the state vector $\mathbf{x}$(k) to obtain a set of $(2n+1)$ sigma points $\chi_i(k|k)$ as presented above in Section (II-A).

The predicted state can be computed by applying the state transition function $f(\cdot)$ to each of the $\chi_i(k|k)$ to obtain a new set of sigma points $\chi_i(k+1|k)$:

$$\chi_i(k+1|k) = f[\chi_i(k|k)] \quad i = 0, ..., 2n+1 \tag{4}$$

Considering the process noise as additive and independent of the state prediction, the predicted mean and covariance of the state, can be computed as follows [22]:

$$\hat{\mathbf{x}}(k+1|k) = \sum_{i=0}^{2n+1} \omega_i.\chi_i(k+1|k) \tag{5}$$

$$\begin{aligned}\mathbf{P}(k+1|k) = &\sum_{i=0}^{2n+1} \omega_i\{\chi_i(k+1|k) - \hat{\mathbf{x}}(k+1|k)\} \\ &\cdot\{\chi_i(k+1|k) - \hat{\mathbf{x}}(k+1|k)\}^T + \mathbf{Q}\end{aligned} \tag{6}$$

The predicted observation (measurement) is computed by applying the observation function h(.) to each of the $\chi_i(k+1|k)$ to obtain a new set of sigma points $\gamma_i(k+1|k)$ as:

$$\gamma_i(k+1|k) = h[\chi_i(k+1|k), \mathbf{u}(k+1)] \qquad i = 0, ..., 2n+1 \tag{7}$$

Considering the measurement noise as additive and independent of the measurement prediction, the predicted mean and covariance of the measurement, can be computed as follows:

$$\hat{\mathbf{y}}(k+1|k) = \sum_{i=0}^{2n+1} \omega_i.\gamma_i(k+1|k) \tag{8}$$

$$\begin{aligned}\mathbf{P}_{yy}(k+1|k) = &\sum_{i=0}^{2n+1} \omega_i\{\gamma_i(k+1|k) - \hat{\mathbf{y}}(k+1|k)\} \\ &\cdot\{\gamma_i(k+1|k) - \hat{\mathbf{y}}(k+1|k)\}^T + \mathbf{R}\end{aligned} \tag{9}$$

The predicted cross correlation is given by:

$$\begin{aligned}\mathbf{P}_{xy}(k+1|k) = &\sum_{i=0}^{2n+1} \omega_i\{\chi_i(k+1|k) - \hat{\mathbf{x}}(k+1|k)\} \\ &\cdot\{\gamma_i(k+1|k) - \hat{\mathbf{y}}(k+1|k)\}^T\end{aligned} \tag{10}$$

*2) Update:* The update step is carried out in the same manner as within the traditional Kalman filter framework. The Kalman gain $L$, for time $t = k+1$ is: $L(k+1) = \mathbf{P}_{xy}(k+1|k).\mathbf{P}_{yy}(k+1|k)^{-1}$

The actual measurement $\mathbf{z}$ can be taken into account, leading to the estimate of the state statistics:

$$\mathbf{x}(k+1) = \hat{\mathbf{x}}(k+1|k) + L.(\mathbf{z} - \hat{\mathbf{y}}) \tag{11}$$

and

$$\mathbf{P}(k+1) = \mathbf{P}(k+1|k) - L.\mathbf{P}_{yy}(k+1|k).L^T \tag{12}$$

### C. The Model of Chan and Vese

Active contours evolving according to edge based and/or region based flows are very commonly used for image segmentation (see [24] and the references therein). The level set representation is the most widely used tool for implementing such geometric curve evolution equations.

Many methods [25], [26], [11] which incorporate geometric and/or photometric (color, texture, intensity) information have been shown to segment images in the presence of noise and clutter. In the present paper we have used the Mumford-Shah functional [9] as modelled by Chan and Vese [10] to obtain the curve evolution equation, which we describe briefly. We seek to minimize the following energy functional:

$$E_{image} = \nu \int_{\Omega} |\nabla H(\Phi)| dx\ dy + \int_{\Omega} (I - c_1)^2 H(\Phi) dx\ dy + \int_{\Omega} (I - c_2)^2 (1 - H(\Phi))\ dx\ dy \tag{13}$$

where $c_1$ and $c_2$ are defined as $c_1 = \frac{\int I(x,y) H(\Phi) dx\ dy}{\int H(\Phi) dx\ dy}$, $c_2 = \frac{\int I(x,y)(1-H(\Phi)) dx\ dy}{\int (1-H(\Phi)) dx\ dy}$ and $H(\Phi)$ is the Heaviside function defined as

$$H(\Phi) = \begin{cases} 1 & if \quad \Phi \geq 0\,, \\ 0 & otherwise \end{cases}$$

$I(x, y)$ is the image and $\Phi$ is the level set function corresponding to the segmenting curve. The above energy functional $E_{image}$ can be minimized using calculus of variations. The Euler-Lagrange equation for minimizing this functional can be implemented by the following gradient descent [10], [9]:

$$\frac{\partial \Phi}{\partial t} = \delta_\epsilon(\Phi) \left[ \nu \text{ div} \left( \frac{\nabla \Phi}{|\nabla \Phi|} \right) - (I - c_1)^2 + (I - c_2)^2 \right] \tag{14}$$

where, $\delta_\epsilon(s) = \frac{\epsilon}{\pi(\epsilon^2 + s^2)}$

### D. Shape Statistics

In [11] the authors apply PCA (principal component analysis) on a set of signed distance functions in order to obtain the major modes of variation of shapes. Let $\Phi_i$ represent the signed distance function corresponding to the curve $C_i$. All the $\Phi_i$'s are aligned using a suitable method of registration [27]. The mean surface, $\mu$, is computed by taking the mean of the signed distance functions, $\mu = \frac{1}{n} \sum \Phi_i$. The variance in shape is computed using PCA, i.e., the mean shape $\mu$ is subtracted from each $\Phi_i$ to create a mean-offset map $\bar{\Phi}_i$. Each such map, $\bar{\Phi}_i$, is placed as a column vector in an $N^d \times n$-dimensional matrix M, where $\Phi_i \in \mathbf{R}^{N^d}$. Using Singular Value Decomposition (SVD), the covariance matrix $\frac{1}{n} M M^T$ is decomposed as:

$$U \Sigma U^T = \frac{1}{n} M M^T \tag{15}$$

where $U$ is a matrix whose column vectors represent the set of orthogonal modes of shape variation and $\Sigma$ is a diagonal matrix of corresponding singular values.

An estimate of a novel shape $\Phi$ of the same class of object (*and registered with the learnt shapes*) can be represented by an $m$-dimensional vector of coefficients, $\alpha = U_m^T(\Phi - \mu)$, where $U_m$ is a matrix consisting of the first m columns of $U$. Given the coefficients $\alpha$, an estimate of the shape $\Phi$,namely $\tilde{\Phi}$, can be obtained as

$$\tilde{\Phi} = U_m \alpha + \mu \tag{16}$$

## III. Implementation

### A. The State Space Model

The authors in [15] separate the motion of an object into two distinct parts: a "global" rigid motion, and a "deformation" which is given by any departure from rigidity. They also show that the overall motion of a moving and deforming object can be described by a set of non-unique rigid motion parameters and a "deformation" function. Accordingly, in this paper, we assume that the "global" motion of an object is given by the translation of its centroid, and any other "deformation" is captured by the curve evolution equation (14) described in the previous section.

We propose to combine the advantages of the unscented Kalman filter and the geometric active contours in order to track both aspects of the motion of an object. A curve being an element of the infinite dimensional space $S^1 \mapsto \mathbb{R} * \mathbb{R}$, a finite dimensional approximation is needed to include the contour into the state space and control it through the Unscented Kalman filter. This finite dimensional approximation is obtained using the method presented in II-D, which results in a projection in an orthogonal PCA base (of finite dimension) and gives access to shape statistics.

In our framework, the state vector is thus composed of the coordinates of the centroid of the object $(x_c, y_c)$ and the curve coordinates in the PCA base ($m$-dimensional coefficient vector $\alpha$), i.e.:

$$\mathbf{x}(k) = \begin{pmatrix} x_c \\ y_c \\ \alpha \end{pmatrix}(k) = \begin{pmatrix} X \\ \alpha \end{pmatrix}(k)$$

Consequently, the dimension of the state vector is $m+2$. The observation space in this model is also a $m+2$-dimensional vector given by:

$$\mathbf{y}(k) = \begin{pmatrix} x_m \\ y_m \\ \beta \end{pmatrix}(k) = \begin{pmatrix} Y \\ \beta \end{pmatrix}(k)$$

where $\beta$ is the $m$-dimensional coefficient vector representing the measurement contour and $(x_m, y_m)$ is the measured position. The predicted covariance matrices for the state $\mathbf{x}$ and the measurement $\mathbf{y}$ can be written as:

$$\mathbf{P}(k+1|k) = \begin{pmatrix} P & 0 \\ 0 & \Sigma \end{pmatrix},\ \mathbf{P}_{yy}(k+1|k) = \begin{pmatrix} P_{yy} & 0 \\ 0 & \Sigma_{yy} \end{pmatrix}$$

where $P$ and $P_{yy}$ are $2 \times 2$ covariance matrices for the centroid co-ordinates and $\Sigma$ and $\Sigma_{yy}$ are $m \times m$ diagonal matrices obtained as given in (15). Note that we have assumed that the centroid location is independent of the deformation in shape. The process noise matrix $\mathbf{Q}$ and measurement noise

$\mathbf{R}$ are assumed to be constant throughout the state evolution process and are given by:

$$\mathbf{Q} = \begin{pmatrix} Q_X & 0 \\ 0 & Q_\Sigma \end{pmatrix}, \mathbf{R} = \begin{pmatrix} R_X & 0 \\ 0 & R_\Sigma \end{pmatrix}$$

### B. Measurement model

The measurement function at time k, $h(\mathbf{X}(k), \mathbf{I}(k))$, where $\mathbf{X}(k)$ is an $(m+2)$-dimensional seed point (corresponding to a curve centered at a certain position), and $\mathbf{I}$(k) is the image that becomes available at time $t = k$, can be described as follows:

1) Build a cloud of *l* points $\mathbf{X}^{(i)}(k)$, for $i \in [|1..l|]$ around $\mathbf{X}(k)$ (these $(m+2)$-dimensional points correspond to curves centered at certain positions). One way to build this cloud of points is to define a fixed set of $(m+2)$ dimensional vectors $\mathbf{S} = \{\mathbf{s}_1, \mathbf{s}_2, ..., \mathbf{s}_l\}$ and to take $\mathbf{X}^{(i)}(k) = \mathbf{X}(k) + \mathbf{s}_i$.
2) Run equation (14), for *r* iterations for each of the $\mathbf{X}^{(i)}(k)$: *r* can be chosen according to the expected dynamics of deformation of the object. This results in a local exploration of both the position and shape spaces in the neighborhood of $\mathbf{X}(k)$.
3) Select the curve with the minimum Chan-Vese energy (best fitting curve) as the measurement: The centroid of the selected curve is then taken as a measurement for the centroid of the system. The projection of the selected curve, using equation (16), provides a measurement of the shape coordinates in the PCA base.

As can be noticed the measurement function $h(\mathbf{X}, \mathbf{I})$ is highly non linear because of the cumulative effects of the curves evolutions, the selection of the best-fitting curve and its projection into the PCA base. This non-linearity of the measurement function justifies the use of the unscented Kalman filter over more classical Kalman filtering approaches in our framework.

### C. Algorithm

Based on the description above, the algorithm can be summarized as follows:

1) Assume the state $\mathbf{x}(k)$ and covariance $\mathbf{P}(k)$ are known, at time $t = k$.
2) Obtain the $2(m+2)+1$ sigma points $\chi_i$ as presented in equation (1).
3) Obtain the state predictions using equation (4) to (6).
4) Obtain the measurements predictions using equation (7) to (9), taking $\mathbf{X}(k+1) = \chi_i(k+1|k)$ (for $i = 0, ..., 2(m+2)+1$) as seed points in the definition of the measurement function presented above, which also take $\mathbf{I}$(k+1) as an argument. Typically, using $l = 1$ (and $\mathbf{s}_1 = 0$), in the definition of $h$ above, seemed to provide reasonable estimates for the predicted measurement statistics, for the data tested.
5) Obtain the actual measurement $\mathbf{z}$ by taking $\mathbf{X}(k+1) = \mathbf{x}(k)$ (for example) as a seed point and apply the measurement function on $\mathbf{I}$(k+1). A typical set $\mathbf{S}$ can be chosen to be:

$$\mathbf{S} = \{ \begin{pmatrix} 0 \\ 0 \\ 0 \\ \vdots \end{pmatrix}, \begin{pmatrix} \pm 3 \\ 0 \\ 0 \\ \vdots \end{pmatrix}, \begin{pmatrix} 0 \\ \pm 3 \\ 0 \\ \vdots \end{pmatrix} \}$$

6) Complete unscented Kalman filtering process by computing equations (10) to (12).

## IV. Experiments

In this section we describe some experiments performed to test the proposed tracking algorithm. Results of applying the proposed method on three image sequences are given below. Geometric active contour implementation was done using the narrow band method [28] and the model of Chan and Vese [10]. In these experiments, the state transition function *f* in equation (2) was chosen to be identity. For each sequence a PCA base of the object to track was computed off-line as described before: A small training set of *s* images was extracted from each sequence and used to compute *m* components representing the possible modes of variation of the tracked object (eigenvector matrix $U_m$).

### A. Fish Sequence

The Fish video demonstrates the tracking ability of the proposed method under large deformations and partial occlusions. This type of deformations are difficult to track using the standard Condensation filter [1]. The number of images in the training set and of principal directions was 8, i.e., $s = m = 8$ (total number of images in the sequence: 356). The tracking was accurate throughout the whole sequence, despite the relatively small number of direction of variations allowed for the shape (Figure 1).

### B. Car Sequence

In this sequence, the car is partially occluded as it passes behind a lamp post. The Chan-Vese model applied to tracking this sequence fails at the occlusion (Figure 2). Including the curve in the state space allows only a few directions of variation in the shape; hence the overall shape of the curve does not vary too much from one frame to the next (Figure 3). The results shown on this figure are for $s = m = 6$. Note that, even though the vector $\alpha$ provides a shape prior with only 6 possible directions of variation, the proposed model can indeed track large deformations or overcome partial occlusions.

### C. Walking Couple Sequence

In the classical Walking Couple video, the difficulty resides in maintaining the identity of each person during tracking: throughout this sequence, the two persons often touch each other and the contour usually leaks from one person to the other and ends up encompassing the two people (Figure 4). The identity of each person can be maintained using the proposed method since for each image, leaks are rejected by projecting the contour onto the PCA base (which constrains the curve to adopt a shape resembling a walking person). For this sequence, the PCA base was computed from

shapes of the man walking (person on the right); $s$ and $m$ were 8 and 6 respectively. The woman (left) was accurately tracked throughout the sequence, highlighting the robustness of the PCA representation (Figure 5).

## V. Limitations and Future Work

In this paper, we combined the advantages of the unscented Kalman filter and geometric active contours to propose a novel method for tracking deformable objects. The proposed method is fast and computationally efficient compared to the one presented in [19]. The proposed algorithm can deal robustly with large deformations, partial occlusions and identity maintenance.

However, the above framework has limitations, which we intend to overcome in our future work. First, prior knowledge of the principal directions of variation is required. Second, shape variation in directions other than the ones represented by $U_m$ cannot be accommodated. One solution is to update $U_m$ with time. We are currently working on including this possibility into our framework.

## References


[1] Andrew Blake and Michael Isard, Eds., *Active Contours*, Springer, 1998.

[2] D. Terzopoulos and R. Szeliski, *Active Vision*, chapter Tracking with Kalman Snakes, pp. 3–20, MIT Press, 1992.

[3] M. Isard and A. Blake, "Condensation – conditional density propagation for visual tracking," *International Journal of Computer Vision*, vol. 29, no. 1, pp. 5–28, 1998.

[4] P. Li, T. Zhang, and B. Ma, "Unscented kalman filter for visual curve tracking," *Image and Vision Computing*, vol. 22, no. 2, pp. 157–164, 2004.

[5] Y. Chen, T. Huang, and Y. Rui, "Parametric contour tracking using unscented kalman filter," *Proceedings of the International Conference on Image Processing*, vol. 3, no. 3, pp. 613–616, 2002.

[6] A. Yuille, D. Cohen, and P. Halliman, "Feature extraction from faces using deformable templates," in *Proc. CVPR*. IEEE, 1989, pp. 104–109.

[7] S. J. Osher and J. A. Sethian, "Fronts propagation with curvature dependent speed: Algorithms based on hamilton-jacobi formulations," *Journal of Computational Physics*, vol. 79, pp. 12–49, 1988.

[8] J. A. Sethian, "A review of recent numerical algorithms for hypersurfaces moving with curvature dependent speed," *J. Differential Geometry*, vol. 31, pp. 131–161, 1989.

[9] D. Mumford and J. Shah, "Optimal approximation by piecewise smooth functions and associated variational problems," *Commun. Pure Applied Mathematics*, vol. 42, pp. 577–685, 1989.

[10] T. Chan and L. Vese, "Active contours without edges," *IEEE Trans. on Image Processing*, vol. 10, no. 2, pp. 266–277, 2001.

[11] M. Leventon, E. Grimson, and O. Faugeras, "Statistical shape influence in geodesic active contours," in *Proc. CVPR*. IEEE, 2000, pp. 1316–1324.

[12] V. Caselles, F. Catte, T. Coll, and F. Dibos, "A geometric model for active contours in image processing," *Numerische Mathematik*, vol. 66, pp. 1–31, 1993.

[13] Marc Niethammer and Allen Tannenbaum, "Dynamic geodesic snakes for visual tracking," in *Proc. CVPR*, 2004, vol. 1, pp. 660–667.

[14] N. Paragios and R. Deriche, "Geodesic active contours and level sets for the detection and tracking of moving objects," *Transactions on Pattern Analysis and Machine Intelligence*, vol. 22, no. 3, pp. 266–280, 2000.

[15] A. Yezzi and S. Soatto, "Deformotion: Deforming motion, shape average and the joint registration and approximation of structures in images," *International Journal of Computer Vision*, vol. 53, no. 2, pp. 153–167, 2003.

[16] J. Jackson, A. Yezzi, and S. Soatto, "Tracking deformable moving objects under severe occlusions," in *Conf. decision and control*, Dec, 2004.

[17] N. Peterfreund, "Robust tracking of position and velocity with Kalman snakes," *IEEE Transactions on Pattern Analysis and Machine Intelligence*, vol. 21, no. 6, pp. 564–569, 1999.

[18] N. Peterfreund, "The velocity snake: deformable contour for tracking in spatio-velocity space," *Computer Vision and Image Understanding*, vol. 73, no. 3, pp. 346–356, 1999.

[19] Y. Rathi, N. Vaswani, A. Tannenbaum, and A. Yezzi, "Particle filtering for geometric active contours with application to tracking moving and deforming objects," in *CVPR 2005*.

[20] S. Julier and J. Uhlmann, "Unscented filtering and nonlinear estimation," *Proceedings of the IEEE*, vol. 92, no. 3, pp. 401–420, 2004.

[21] S. Julier and J. Uhlmann, "A new method for the nonlinear transformation of means and covariances in filters estimators," *IEEE Transactions on Automatic Control*, vol. 45, no. 3, pp. 477–482, 2000.

[22] R. van der Merwe and E. Wan, "The square-root unscented kalman filter for state and parameter estimation," *Proceedings of the International Conference on Accoustics, speech, and Signal Processing(ICASSP)*, 2001.

[23] R. van der Merwe and E. Wan, "The unscented kalman filter for nonlinear estimation," *Proceedings of IEEE Symposium*, 2000.

[24] Guillermo Sapiro, Ed., *Geometric Partial Differential Equations and Image Analysis*, Cambridge Press, 20010.

[25] M. Rousson and N. Paragios, "Shape priors for level set representations," in *Proceedings of European Conference on Computer Vision*, 2002, pp. 78–92.

[26] A. Tsai and Anthony Yezzi, "Model-based curve evolution technique for image segmentation," in *Proceedings of Computer Vision and Pattern Recognition*, vol. 1.

[27] T. Cootes, C. Beeston, G.Edwards, and C. Taylor, "Unified framework for atlas matching using active appearance models," in *Int'l Conf. Information Processing in Med. Imaging*. Springer-Verlag, 1999, pp. 322–333.

[28] J. A. Sethian, *Level Set Methods and Fast Marching Methods*, Cambridge University Press, 2nd edition, 1999.

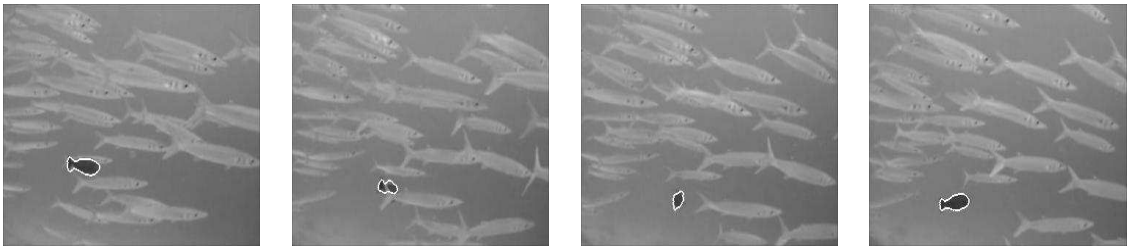

(a) Frame 110 (b) Frame 175 (c) Frame 195 (d) Frame 219

Fig. 1. Fish Sequence: Tracking with the proposed method

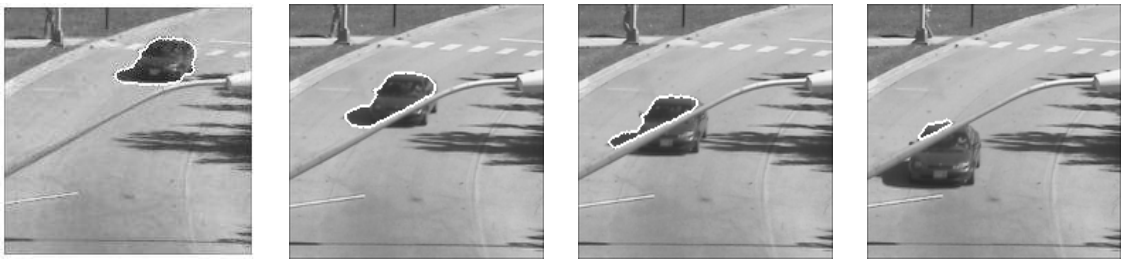

(a) Frame 20 (b) Frame 40 (c) Frame 50 (c) Frame 67

Fig. 2. Car Sequence: Tracking with Chan-Vese model alone - Obstacle cannot be handled

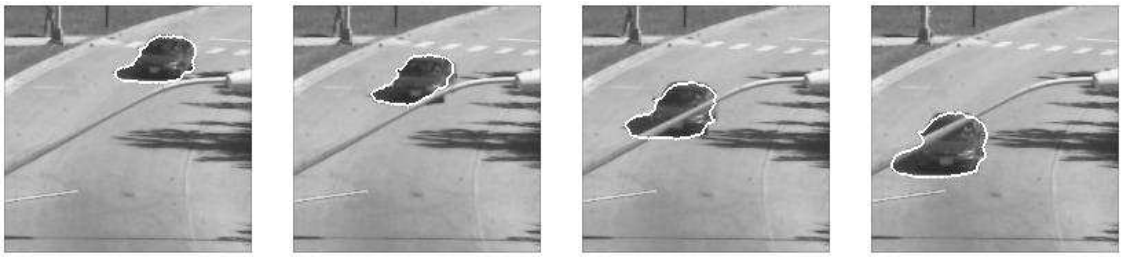

(a) Frame 20 (b) Frame 34 (c) Frame 50 (d) Frame 65

Fig. 3. Car Sequence: Tracking with the proposed method

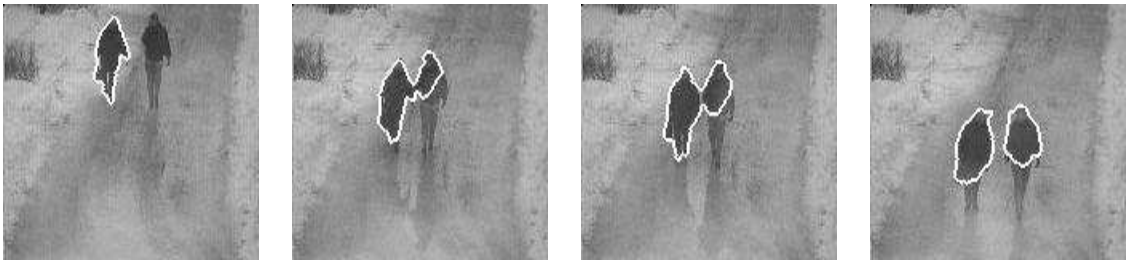

(a) Frame 3 (b) Frame 11 (c) Frame 13 (d) Frame 20

Fig. 4. Walking Couple Sequence: Tracking with Chan-Vese model - Identity cannot be maintained

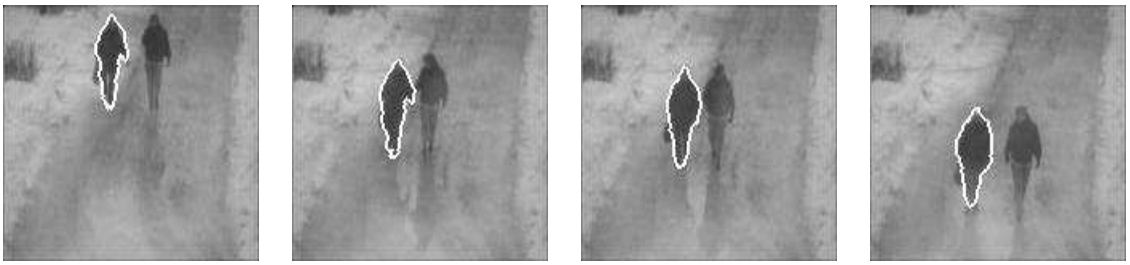

(a) Frame 3 (b) Frame 11 (c) Frame 13 (d) Frame 20

Fig. 5. Walking Couple Sequence: Tracking with the proposed method